

# Effect of cooling rate on achieving thermodynamic equilibrium in uranium–plutonium mixed oxides



Romain Vauchy <sup>a, b, \*</sup>, Renaud C. Belin <sup>b</sup>, Anne-Charlotte Robisson <sup>b</sup>, Fiqiri Hodaj <sup>c, d</sup>

<sup>a</sup> CEA, DEN, DTEC, Marcoule, 30207, Bagnols-sur-Cèze, France

<sup>b</sup> CEA, DEN, DEC, Cadarache, 13108, Saint-Paul-lez-Durance, France

<sup>c</sup> Univ. Grenoble Alpes, SIMAP, F-38000, Grenoble, France

<sup>d</sup> CNRS, Grenoble INP, SIMAP, F-38000, Grenoble, France

## ARTICLE INFO

### Article history:

Received 24 July 2015

Received in revised form

23 November 2015

Accepted 25 November 2015

Available online 30 November 2015

### Keywords:

High temperature X-ray diffraction

Thermodynamic equilibrium

Phase diagram

U–Pu–O

Uranium

Plutonium

Mixed oxide

Nuclear fuel

MOX

Phase separation

Miscibility gap

Lattice expansion

SFR

## ABSTRACT

*In situ* X-ray diffraction was used to study the structural changes occurring in uranium–plutonium mixed oxides  $U_{1-y}Pu_yO_{2-x}$  with  $y = 0.15; 0.28$  and  $0.45$  during cooling from 1773 K to room-temperature under He + 5% H<sub>2</sub> atmosphere. We compare the fastest and slowest cooling rates allowed by our apparatus *i.e.* 2 K s<sup>-1</sup> and 0.005 K s<sup>-1</sup>, respectively. The promptly cooled samples evidenced a phase separation whereas samples cooled slowly did not due to their complete oxidation in contact with the atmosphere during cooling. Besides the composition of the annealing gas mixture, the cooling rate plays a major role on the control of the Oxygen/Metal ratio (O/M) and then on the crystallographic properties of the  $U_{1-y}Pu_yO_{2-x}$  uranium–plutonium mixed oxides.

© 2015 Elsevier B.V. All rights reserved.

## 1. Introduction

Uranium–plutonium mixed oxides  $U_{1-y}Pu_yO_{2-x}$  with high amounts of plutonium are envisaged as fuel for future Sodium-cooled Fast Reactors (SFRs) [1]. Although the exact nature of SFRs' nuclear fuels is still under consideration, general trends are already defined. The fuel will be oxygen-hypostoichiometric uranium–plutonium mixed oxides ( $O/(U + Pu) = O/M$  ratio < 2.0) with a plutonium content ranging between  $0.20 \leq y \leq 0.30$ . Furthermore, depending upon the fabrication route and raw materials used for nuclear fuel processing, *i.e.* upon cation distribution homogeneity, local high and low Pu content zones might be present within the

fuel. These local variations in the plutonium content ( $y$ ) might go up to ~0.45 or down to ~0.15 in the case of co-converted powders [2]. In the  $UO_2$ – $PuO_2$ – $Pu_2O_3$  sub-system, corresponding to the domain of interest for nuclear fuel for future SFRs,  $U_{1-y}Pu_yO_{2-x}$  mixed oxides with high plutonium content ( $y > 0.20$ ) are multiphase at room temperature [2–16].

In this system, a miscibility gap exists and is composed of two fluorite face-centered cubic *fcc* phases for the lower Pu contents ( $0.20 \leq y \leq 0.45$ ) and of an *fcc* phase in equilibrium with an  $\alpha$ - $Pu_2O_3$ -type body centred cubic *bcc* phase in the higher plutonium content range [5–9]. The two phases constituting the hypostoichiometric mixed oxides exhibit different oxygen content and are so called “high-oxygen” and “low-oxygen” phases, respectively [13–16].

The effect of fast cooling rate on phase equilibria, O/M ratio and microstructure of  $U_{1-y}Pu_yO_{2-x}$  was presented in previous studies

\* Corresponding author. CEA, DEN, DTEC, Marcoule, 30207, Bagnols-sur-Cèze, France.

E-mail address: [romain.vauchy@cea.fr](mailto:romain.vauchy@cea.fr) (R. Vauchy).

[13,14]. However, to our knowledge, very slow cooling rates as those used in this work ( $0.005 \text{ K s}^{-1}$ ), have never been studied by high-temperature X-ray diffraction (HT-XRD). Therefore, the aim of the present work was to investigate the variations in O/M ratio and structural changes of uranium–plutonium mixed oxides  $\text{U}_{1-y}\text{Pu}_y\text{O}_{2-x}$  with  $y = 0.15$ ;  $0.28$  and  $0.45$  when subjected to very slow cooling rates under the same thermodynamic conditions as in previous studies within the scope of comparing the associated results [13,14]. Furthermore, lattice contraction of the three considered uranium–plutonium mixed oxides was also investigated during cooling.

## 2. Materials and methods

### 2.1. Materials

The uranium dioxide powder was produced by a wet fabrication route based on the formation of ammonium diuranate (ADU) from uranyl nitrate precipitated with ammonia. The obtained particles were then atomized, dried and calcinated, leading to spherical-shaped agglomerates of around  $20 \mu\text{m}$ . Plutonium dioxide powder was produced by precipitation of a plutonium nitrate solution with oxalic acid to form plutonium oxalate. The particles were heated in air at  $923 \text{ K}$  and parallelepiped-shaped  $\text{PuO}_2$  particles were obtained with an average size of  $15 \mu\text{m}$ .

Uranium–plutonium mixed oxide samples  $\text{U}_{1-y}\text{Pu}_y\text{O}_2$  were obtained by mixing  $\text{UO}_2$  (respectively  $1-y = 0.85$ ,  $0.72$  and  $0.55$ ) with  $\text{PuO}_2$  (respectively  $y = 0.15$ ,  $0.28$  and  $0.45$ ). Each of these three mixtures was then micronized by co-milling in order to improve the U–Pu distribution in the final material. Then, each of the powders was pressed into  $\sim 2 \text{ g}$  pellets at  $\sim 400 \text{ MPa}$ , sintered at  $2023 \text{ K}$  for  $24 \text{ h}$  under  $\text{Ar} + 5\% \text{ H}_2 + \sim 1500$  volume per million (vpm)  $\text{H}_2\text{O}$  and slowly cooled at  $\sim 0.01 \text{ K s}^{-1}$ . These conditions were determined according to the thermodynamic model proposed by Guéneau et al. [17] to obtain stoichiometric compounds (Oxygen/Metal = 2.000) at room temperature. The obtained pellets were free from defects (cracks, exacerbated pores ...) with a high density ( $>95\%$  of the theoretical density). The average grain size was determined by observing the microstructure of polished dense pellets after chemical etching and was equal to  $30\text{--}40 \mu\text{m}$  regardless of the Pu content (Fig. 1). The detailed fabrication process is described elsewhere [18].

### 2.2. High-temperature X-ray diffraction

XRD measurements were performed at ambient pressure and various temperatures with a Bragg–Brentano  $\theta$ – $\theta$  BRUKER D8 Advance X-ray diffractometer using copper radiation from a conventional tube source ( $K\alpha_1 + K\alpha_2$  radiation;  $\lambda = 1.5406$  and  $1.5444 \text{ \AA}$ ) at  $40 \text{ kV}$  and  $40 \text{ mA}$ , and a LynX'Eye fast-counting PSD detector with an opening angle of  $3^\circ 2\theta$ . The entire apparatus

resides in its own custom-built nitrogen-filled glove-box dedicated to handling of nuclear materials at the LEFCA facility (CEA Cadarache, France). The diffractometer is equipped with heating stage from MRI PhysikalischeGeräte GmbH TC-Radiation of volume  $0.5 \text{ L}$ , allowing heating of the sample up to  $2273 \text{ K}$ . Under reducing atmosphere, it uses both a molybdenum strip as a direct heater and a tantalum radiant heater. After each setup adjustment, a temperature calibration was carried out in steps of  $100 \text{ K}$  from room-temperature to  $1973 \text{ K}$ , using tungsten powder (ALDRICH, 99.999%). Tungsten lattice parameters as a function of temperature were taken from Refs. [19,20]. Temperature calibration was repeated several times. Calibration results were then compared, giving a constant temperature uncertainty of  $15 \text{ K}$  across the temperature range used. Rocking curve and displacement corrections were systematically applied to take into account the angular position and displacement of the strip. Full powder diffraction patterns were obtained by scanning from  $22^\circ$  to  $145^\circ 2\theta$  in isothermal conditions at each temperature. A counting time of  $0.3 \text{ s}$  per step and step-intervals of  $0.02^\circ 2\theta$  were chosen.

### 2.3. HT-XRD data refinements

Contrary to some of our previous studies [13,14], the angular range of the full powder diffraction patterns made it possible to determine lattice parameters and phase fractions as a function of time and temperature. Powder patterns were refined according to the Pawley [21] or the Rietveld [22] methods, based on the fundamental parameter approach [23] available in the DIFFRACplus TOPAS V4 software package [24]. The line profile shapes are described by convoluting the wavelength distribution of the emission profile, considering the instrument geometry and aberrations and physical properties of the sample. The microstructural contributions were simulated with a physical broadening function added to the refinement. As the fundamental parameter approach adequately fits the instrumental contributions to the observed peak profiles (geometry, tube type and slit system), a standard refinement of sample effects such as crystallite size can be performed. The background was approximated by a Chebyshev polynomial function with three terms. The refinement procedure first considers the zero detector and background parameters, then lattice parameter and crystallite size. The uncertainty on the lattice parameter is estimated less than  $0.001 \text{ \AA}$  at any temperature.

### 2.4. Atmosphere control

The oxygen partial pressure  $p\text{O}_2$  of the gas used here ( $\text{He} + 5\% \text{ H}_2 + z \text{ vpm H}_2\text{O}$ ), controlled *via* its moisture content  $z$ , was generated by a SETNAG yttria stabilized zirconia oxygen pump operating at  $1073 \text{ K}$ . Furthermore,  $p\text{O}_2$  was also monitored using a similar device operating at  $948 \text{ K}$ . The moisture content  $z$  of the gas was also measured and recorded using a VAISALA DM70 capacitive

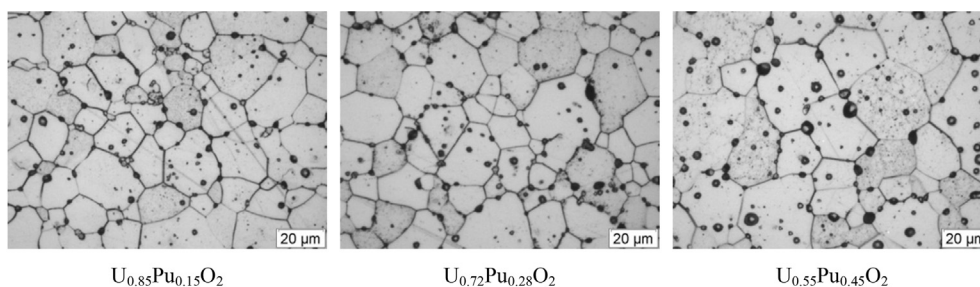


Fig. 1. Microstructures of  $\text{U}_{1-y}\text{Pu}_y\text{O}_2$  mixed oxides after chemical etching.

Download English Version:

<https://daneshyari.com/en/article/1564786>

Download Persian Version:

<https://daneshyari.com/article/1564786>

[Daneshyari.com](https://daneshyari.com)